Clinical Rheumatology (2026) 45:1981–1992
https://doi.org/10.1007/s10067-025-07910-1

ORIGINAL ARTICLE

Diagnostic value of lung ultrasound vs. quantitative computed tomography in connective tissue disease–associated interstitial lung disease: a preliminary study

Xiaokun Xin[1] · Meng Huang[2] · Hui Yuan[3] · Li Zhang[1] · Shan Dang[4] · Guoqin Huang[2] · Nan Yu[1,4]

Received: 20 June 2025 / Revised: 18 November 2025 / Accepted: 21 December 2025 / Published online: 15 January 2026
© The Author(s), under exclusive licence to International League of Associations for Rheumatology (ILAR) 2026

Abstract

Purpose To evaluate the utility of modified lung ultrasound (LUS) and quantitative computed tomography (QCT) in assessing connective tissue disease–associated interstitial lung disease (CTD-ILD) and their correlations with high-resolution computed tomography (HRCT) of the chest.

Methods Between October 2023 and 2024, 77 hospitalized CTD patients (57 CTD-ILD, 20 controls) who had undergone or were scheduled for chest HRCT also received LUS during their hospitalization, ensuring both assessments were completed within 1 week. The LUS and HRCT results were evaluated using modified LUS scores and Warrick scores, respectively. HRCT results were analyzed quantitatively using the "Dexin-FACT" automated analysis software.

Results Significant differences were observed in all LUS parameters and most QCT parameters between groups ($P < 0.01$), with significant correlations to ILD severity stratification ($P < 0.05$). Univariate analysis identified modified LUS scores, $LAA_{-600\sim-250}\%$, and the TAV/TNV ratio (the ratio of lumen area to number of blood vessels around the bronchus with a 2 mm diameter in the lower lobe of the lung) as being associated with ILD ($P < 0.01$). After initial adjustment for age, gender, and BMI, the modified LUS scores demonstrated a significant association with CTD-ILD (OR = 1.94, 95% CI 1.26–2.98). Notably, this association was substantially strengthened in the fully adjusted model controlling for a broader set of clinical confounders, including smoking, disease duration, complications, and CTD type (aOR = 3.62, 95% CI 1.58–8.29), confirming it as the strongest independent predictor compared to $LAA_{-600\sim-250}\%$ and TAV/TNV. The modified LUS scores showed excellent diagnostic concordance with the Warrick scores (AUC = 0.960), outperforming $LAA_{-600\sim-250}\%$ (AUC = 0.873).

Conclusion Modified LUS shows potential as a practical tool for CTD-ILD detection, outperforming QCT parameters in diagnostic agreement with HRCT. These preliminary findings support LUS as an effective adjunct for CTD-ILD assessment.

Key Points

- *Modified lung ultrasound scores outperformed traditional ultrasound metrics in distinguishing connective tissue disease–associated interstitial lung disease severity and showed the strongest predictive association with disease presence.*
- *Significant differences in lung ultrasound and quantitative CT parameters were observed between connective tissue disease–associated interstitial lung disease and non-interstitial lung disease groups, correlating with disease progression and severity stratification.*
- *Modified lung ultrasound demonstrated superior specificity to quantitative CT in detecting connective tissue disease–associated interstitial lung disease, highlighting its potential as a practical, non-invasive adjunct to HRCT.*

Keywords B-lines · Connective tissue diseases · Interstitial lung disease · Lung ultrasound · Quantitative computed tomography

Summary statement Modified lung ultrasound demonstrates strong diagnostic concordance with HRCT in assessing connective tissue disease–associated interstitial lung disease, outperforming quantitative CT parameters, and may serve as a practical adjunct tool for clinical evaluation.

Abbreviations

LUS	Lung ultrasound
QCT	Quantitative computed tomography
CTD-ILD	Connective tissue disease–associated interstitial lung disease

Extended author information available on the last page of the article

SHOUT
SHARE
IT

$LAA_{-600–250}$%	Percentage of lung volume with CT number from − 600 to − 250 HU in the total lung volume
TNV	The number of surrounding vessels
TAV	Cross area of surrounding vessels
TAV/TNV	The ratio of lumen area to number of blood vessels around the bronchus with a diameter of 2 mm in the lower lobe of the lung
TLV	Total lung volume
TPVV	Total pulmonary vascular volume
TPVV%	The ratio of total pulmonary vascular volume to total lung volume

Introduction

Interstitial lung disease (ILD) is the most prevalent and clinically significant pulmonary complication of connective tissue diseases (CTD), serving as an independent predictor of poor prognosis and frequently presenting as the initial manifestation in 30%–40% of CTD cases [1, 2]. Epidemiological studies reveal that ILD occurs across various CTD subtypes, including rheumatoid arthritis, systemic sclerosis, systemic lupus erythematosus, polymyositis/dermatomyositis, Sjögren's syndrome, and mixed connective tissue disease, with markedly heterogeneous incidence rates ranging from 5 to 65% [3]. The clinical course of CTD-ILD demonstrates substantial variability, ranging from prolonged stability to acute exacerbations that progress to fatal respiratory failure [1, 4]. This unpredictable disease trajectory highlights the urgent need for effective monitoring systems with high sensitivity and reproducibility to support personalized, precision management [5].

In recent years, lung ultrasound (LUS) has garnered increasing attention for diagnosing and monitoring CTD-ILD, demonstrating significant sensitivity and an excellent negative predictive value comparable to the gold standard of high-resolution computed tomography (HRCT) [3, 6]. Its radiation-free nature, operational convenience, cost-effectiveness, and real-time bedside assessment capabilities make it an ideal tool for ILD screening and follow-up. However, standardized LUS diagnostic criteria for CTD-ILD have not yet been established [7]. Traditional LUS evaluation primarily relies on B-lines—vertical hyperechoic artifacts that result from reverberation phenomena at alveolar-interstitial interfaces due to differences in acoustic impedance [8]. Studies quantifying B-lines with LUS for ILD show good diagnostic accuracy, high sensitivity, and a strong correlation with HRCT findings [9–12]. However, clinical observations suggest that 85% of ILD patients also exhibit pleural line abnormalities (such as thickening, irregularity, or fragmentation) [13, 14], indicating limitations in using B-line evaluation alone. Growing evidence suggests that integrated scoring systems combining B-line quantification with pleural lines analysis can significantly improve diagnostic performance [15, 16]. Therefore, some researchers advocate that CTD-ILD evaluation should be based not only on B-line counts but also incorporate other sonographic signs [16]. In this study, we adopted a widely used standardized 12-region scanning protocol and developed a modified LUS score that integrates both B-lines and pleural line assessments.

Additionally, there is a paucity of comparative studies assessing different LUS scoring systems against CT and quantitative CT (QCT) evaluations. While QCT is also a well-validated tool for identifying early-stage CTD-ILD and monitoring its progression—providing objective quantification of structural, interstitial, and microvascular changes [15, 17, 18]—direct comparisons of different LUS scoring systems against these robust CT and QCT benchmarks remain scarce. Therefore, this study aims to validate the accuracy of a modified LUS scoring system—incorporating B-line patterns, pleural line characteristics, and associated complications—against HRCT for detecting CTD-ILD, and to compare its performance with QCT parameters. We hypothesize that the modified LUS scores can reliably detect and assess the severity of CTD-ILD, potentially outperforming individual QCT parameters in diagnostic performance.

Methods

This prospective study enrolled 77 inpatients diagnosed with CTD who had undergone or were scheduled for HRCT scans at our institution between October 2023 and April 2024. All participants underwent concurrent LUS and HRCT examinations within 1 week to ensure temporal consistency for diagnostic comparisons. The study protocol was approved by the Ethics Committee of the Affiliated Hospital of Shaanxi University of Chinese Medicine (Approval No. SZFYIEC-BA-2024–20), and written informed consent was obtained from all participants after a thorough explanation of the research objectives and procedures. Comprehensive demographic data, including patient names, gender, age, body mass index (BMI), smoking history, and disease duration, were systematically collected, along with clinical profiles and laboratory parameters. These variables were later correlated with LUS findings through integrated analysis.

The inclusion criteria were as follows: (1) confirmed diagnosis of any CTD according to the ACR/EULAR 2013 classification criteria [19–23] and (2) voluntary participation in the study with signed informed consent. The exclusion criteria included the following: (1) coexisting pulmonary diseases, including severe pulmonary infection, idiopathic pulmonary fibrosis, lung tumors, radiation-induced lung

Table 1 Modified lung ultrasound scoring system

Ultrasound findings	Score per region	Ultrasound findings	Score per region
Number of B-lines		Complication signs	
None	0	A-line	0
< 4 lines	1	Present	4
4–6 lines	2	Pulmonary consolidation	
> 6 lines or white lung	3	Absent	0
Pleural line		Present	4
Smooth, clear	0		
Thickened, blurred	1		
Irregular with occasional breaks	2		
Discontinuous ("fragmented")	3		

The score for each lung region is calculated by summing the scores from B-lines, pleural lines, and complication assessments. The total lung score is the sum of scores from all 12 lung regions

injury, or prior lung surgery; (2) other causes of interstitial lung disease, such as heart failure, severe valvular heart disease, or renal failure; (3) inability to cooperate with relevant examinations (e.g., CT scans and ultrasound), incomplete clinical data, or poor image quality; and (4) pregnancy.

LUS assessment

LUS examinations were performed using a portable color Doppler ultrasound system (Mindray M9, Mindray Medical International Ltd). A convex array probe (2–5 MHz) was used for B-lines assessment, while a linear array probe (3–9 MHz) was employed for pleural line evaluation. Both probes were used in combination to assess subpleural and pleural conditions. A standardized 12-region scanning protocol was followed, covering the anterior, lateral, and posterior chest walls. The probe was positioned perpendicular to the ribs to scan the intercostal spaces. The anterior and lateral chest walls were examined with the patient in a supine position, while the posterior chest walls were examined in a seated position. A semi-quantitative scoring system was applied: B-lines were scored as 0 (A-lines, normal ventilation), 1 (discrete B-lines, mild ventilation reduction), 2 (confluent B-lines, alveolar infiltration), or 3 (lung consolidation/atelectasis, complete ventilation loss). Pleural line abnormalities were scored as 0 (smooth), 1 (thickened), 2 (irregular/coarse), or 3 (discontinuous/fragmented). To enhance diagnostic accuracy, a modified ultrasound scoring system (Table 1) categorized ILD findings into two groups: (1) typical findings: B-lines and pleural line abnormalities; (2) complication-related findings: pleural effusion and A-lines. All examinations were performed by lung ultrasound-trained physicians who were blinded to HRCT results, ensuring objective assessment.

CT analysis

Chest CT images were obtained using a GE (Discovery 750HD, GE Healthcare, Milwaukee, WI, USA) CT scanner. The scanning parameters were as follows: tube voltage 120 kV, automated tube current modulation (with a noise index of 25), rotation time 0.5 s, and a pitch of 0.984. The raw data were reconstructed into axial images with a slice thickness of 1.0 mm at an interval of 0.625 mm for analysis. Two thoracic radiologists, blinded to the LUS results, independently assessed ILD severity using the Warrick scoring system [24, 25] (Table 2) on HRCT, demonstrating good interobserver agreement (kappa = 0.82). Following this, the CT images were analyzed further using the "Dexin-FACT, Xi'an" platform. This software utilizes a three-dimensional adaptive boundary marching algorithm to extract comprehensive lung data, automatically calculating parameters such as total lung volume (TLV), total pulmonary vascular

Table 2 Warrick scoring criteria

Category	HRCT findings	Score
Lesion type	Ground-glass opacity	1
	Pleural thickening with irregular margins	2
	Septal thickening and subpleural band-like opacities	3
	Reticular pattern	4
	Honeycombing	5
Extent of lesion	1–3 segments	1
	4–9 segments	2
	> 9 segments	3

Semi-quantitative grading of Warrick score: grade 1 (mild): 1–10 points; grade 2 (moderate): 11–20 points; grade 3 (severe): 21–30 points

Table 3 Baseline characteristics of the study population

Parameters	CTD-ILD	CTD without ILD	All	*P* values
Sample size, *n* (%)	57 (74.0)	20 (26.0)	77	
Gender, *n* (%)				0.077
Female	40 (70.2)	18 (90.0)	58 (75.3)	
Male	17 (29.8)	2 (10.0)	19 (24.7)	
Age, year	65.0 (54.5–71.0)	54.0 (40.3–57.8)	60 (53.0–69.5)	0.000
Height (cm)	160.0 (155.0–168.0)	160.0 (156.3–166.8)	160.0 (155.0–167.5)	0.880
Weight (kg)	60.0 (53.5–65.5)	57.5 (55.0–61.0)	59.0 (54.5–64.5)	0.334
Body mass index (kg/m^2)	22.94 ± 3.50	22.09 ± 1.89	22.75 ± 3.26	0.183
Smoking, *n* (%)				0.279
No	49 (86.0)	19 (95.0)	68 (88.3)	
Yes	8 (14.0)	1 (5.0)	9 (11.7)	
Type of CTD, *n* (%)				
Rheumatoid arthritis	37 (64.9)	16 (80.0)	53 (68.8)	
Systemic ilupus erythematosus	4 (7.0)	0	4 (5.2)	
Systemic sclerosis	6 (10.5)	0	6 (7.8)	
Sjogren's syndrome	6 (10.5)	3 (15.0)	9 (11.7)	
Polymyositis/dermatomyositis	1 (1.8)	0	1 (1.3)	
Mixed CTD	3 (5.3)	1 (5.0)	4 (5.2)	
Duration, month	84.0 (18.0–204.0)	66.0 (12.0–120.0)	72.0 (12.0–144.0)	0.215
Complication				
Osteoporosis	13 (22.8)	4 (20.0)	17 (22.1)	
Pulmonary hypertension	3 (5.3)	0 (0)	3 (3.89)	
LUS assessments				
Total B-lines scores	12.0 (4.0–18.5)	0 (0–2.0)	5.0 (2.0–16.0)	0.000
Total pleura-lines scores	10.0 (6.0–17.0)	2.0 (0–4.0)	8.0 (4.0–16.0)	0.000
Modified LUS scores	25.0 (9.5–35.0)	3.5 (0.5–5.0)	13.0 (5.0–32.0)	0.000
QCT analysis				
TLV	3380.43 ± 1134.16	4171.10 ± 898.24	3585.75 ± 1127.52	0.006
TPVV	127.26 ± 44.69	143.36 ± 26.78	131.39 ± 41.24	0.061
TPVV %	3.90 ± 1.14	3.53 ± 0.49	3.78 ± 1.01	0.031
$LAA_{-600–250}$%	9.34 (6.82–15.03)	5.81 (4.29–6.46)	7.76 (6.15–11.95)	0.000
TNV	15.36 ± 7.18	17.03 ± 3.65	15.77 ± 6.42	0.184
TAV	115.93 ± 72.21	163.72 ± 51.34	128.31 ± 70.28	0.008
TAV/TNV	7.35 ± 2.87	9.70 ± 2.85	7.96 ± 3.03	0.002

CTD-ILD connective tissue disease–associated interstitial lung disease, *LUS* lung ultrasound, *QCT* quantitative computed tomography, *TLV* total lung volume, *TPVV* total pulmonary vascular volume, *TPVV%* the ratio of total pulmonary vascular volume to total lung volume, $LAA_{-600–250}$% percentage of lung volume with CT number from − 600 to − 250 HU in the total lung volume, *TNV* the number of surrounding vessels, *TAV* cross area of surrounding vessels, *TAV/TNV* the ratio of lumen area to number of blood vessels around the bronchus with a diameter of 2 mm in the lower lobe of the lung

volume (TPVV), and the percentage of the total lung volume (TPVV%).

The lung density histogram module was employed to measure the percentage of lung volume with CT values between − 600 and − 250 Hounsfield units relative to the total lung volume ($LAA_{-600–250}$%) [26], which serves as an index for pulmonary fibrosis. Additionally, the software segments bronchi and pulmonary vascular trees based on principal curvatures and directions, generating three-dimensional visualizations of these structures. Using the automatic measurement module for pulmonary vessels, bronchi with a diameter of 2 mm in the lower lobes of both lungs were selected, and the number of surrounding vessels (TNV) and lumen area (TAV) within a viewing area of 80 mm^2 were quantified. To account for physiological anatomical variations, the ratio of lumen area

Table 4 Comparative analysis of lung ultrasound, CT-derived, and vascular metrics across mild, moderate, and severe disease groups

Parameters	Mild group (1)	Moderate group (2)	Severe group (3)	*P* values			
	$n=28$	$n=18$	$n=11$	(1) vs. (2)	(1) vs. (3)	(2) vs. (3)	All
Total B-line scores	4.00 (3.00, 12.75)	12.50 (6.75, 20.25)	19.00 (12.00, 24.00)	0.005	< 0.001	0.108	< 0.001
Total pleura-line scores	7.00 (4.00, 10.75)	12.00 (7.50, 19.25)	18.00 (17.00, 20.00)	0.015	< 0.001	0.029	< 0.001
Modified LUS scores	12.50 (6.25, 25.00)	26.50 (15.00, 38.25)	38.00 (34.00, 42.00)	0.006	< 0.001	0.035	< 0.001
$LAA_{-600\sim-250}\%$	7.80 (6.41, 11.70)	8.89 (6.50, 18.20)	15.50 (11.92, 17.24)	0.330	0.001	0.019	0.004
TNV	16.21 ± 6.06	16.72 ± 6.85	10.82 ± 8.81	0.559	0.003	0.002	0.004
TAV	126.13 ± 68.06	137.91 ± 75.46	53.83 ± 39.59	0.808	0.032	0.029	0.061
TAV/TNV	7.60 ± 2.86	7.95 ± 2.10	5.74 ± 3.58	0.683	0.067	0.044	0.105
TLV	3473.27 ± 925.26	3510.99 ± 1389.74	2930.14 ± 1153.51	0.913	0.183	0.186	0.346
TPVV	147.98 ± 39.78	122.45 ± 34.14	82.18 ± 38.19	0.029	< 0.001	0.007	< 0.001
TPVV%	4.38 ± 0.99	3.77 ± 1.10	2.76 ± 0.63	0.040	< 0.001	0.009	< 0.001

LUS lung ultrasound, $LAA_{-600-250}\%$ percentage of lung volume with CT number from − 600 to − 250 HU in the total lung volume, *TNV* the number of surrounding vessels, *TAV* cross area of surrounding vessels, *TAV/TNV* the ratio of lumen area to the number of blood vessels around the bronchus with a diameter of 2 mm in the lower lobe of the lung, *TLV* total lung volume, *TPVV* total pulmonary vascular volume, *TPVV%* the ratio of total pulmonary vascular volume to total lung volume

to the number of surrounding vessels in 2 mm bronchi in the lower lobes (TAV/TNV) was also calculated.

Statistical analysis

Statistical analysis was performed using SPSS 26.0 and GraphPad Prism 9.5. Continuous variables were expressed as mean ± standard deviation for normally distributed data or median with interquartile range for non-normally distributed data. Categorical variables were presented as frequencies and percentages. The differences in LUS parameters between ILD and non-ILD groups were analyzed using the Mann–Whitney *U* test. Binomial logistic regression analysis, both unadjusted and adjusted for potential confounders, was performed to calculate the odds ratios (OR) for ILD associated with a 1/10 SD increase in the modified LUS and QCT parameters. Non-parametric tests were employed to evaluate the differences in modified LUS scores across various subgroups of CTD-ILD. The diagnostic efficacy of the three scoring methods for CTD-ILD was analyzed using receiver operating characteristic (ROC) curves, and the diagnostic performance of LUS and QCT was compared. A 95% confidence interval (CI) and a P value < 0.05 were considered statistically significant.

Results

Baseline characteristics

The characteristics of the study population are shown in Table 3. The study included 77 patients, of whom 57 were in the CTD-ILD group and 20 in the CTD-non-ILD group. The median age was 60 years (IQR 53.0–69.5), and the median disease duration was 72 months (IQR 12.0–144.0). The cohort was predominantly female (75.3%), with rheumatoid arthritis (RA) being the most common CTD (68.8%).

Differences in parameters among different groups

Patients with CTD-ILD were older and exhibited significantly higher lung ultrasound scores compared to the CTD-non-ILD controls, including total B-lines scores, pleural lines scores, and modified LUS scores (all $P < 0.001$). CTD-ILD patients also demonstrated reduced TLV and TPVV, while showing elevated TPVV% and $LAA_{-600\sim-250}\%$ (Table 3).

Among severe CTD-ILD patients ($n=11$), there were significantly higher ultrasound metrics (B-lines scores, pleural lines scores, modified LUS scores), a progressive reduction in TPVV%, and an increase in $LAA_{-600\sim-250}\%$ compared to mild cases (all $P < 0.05$). Additionally, severe cases had lower TAV/TNV, TNV, and TAV, while $LAA_{-950}\%$ and TLV remained unchanged (Table 4).

LUS assessment: comparison of three ultrasound scores

All ultrasound scores—total B-lines scores, pleura-lines scores, and modified LUS scores—effectively differentiated CTD-ILD severity (all $P < 0.001$) (Fig. 1). Among them, modified LUS scores demonstrated the strongest discriminative capacity (AUC: 0.92), outperforming total B-lines scores (AUC: 0.85) and pleura-lines scores (AUC: 0.81) in ROC analysis (Fig. 2). The DeLong test revealed that the modified LUS score significantly outperformed the pleura-line score ($P=0.020$) (Table 6).

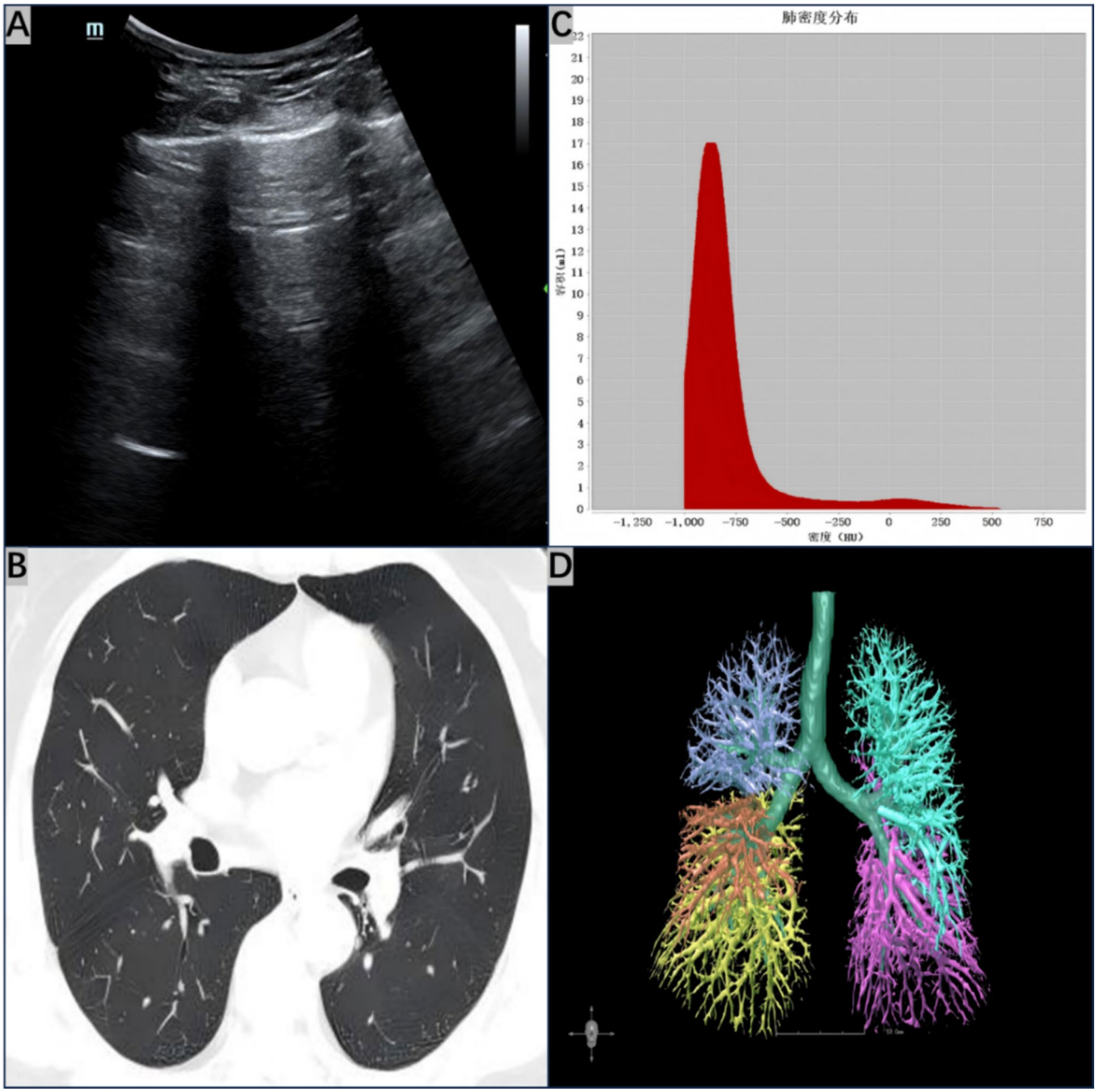

Fig. 1 Images of LUS, HRCT, and QCT in a CTD patient without ILD. **A**–**D** CTD-non-ILD case: **A** normal A-lines on LUS, **B** unremarkable HRCT, and **C**, **D** preserved normal density distribution and bronchovascular architecture on QCT. CTD, connective tissue disease; ILD, interstitial lung disease; LUS, lung ultrasound; HRCT, high-resolution CT; QCT, quantitative CT

LUS assessment compared with QCT: effective parameters

Univariable analysis identified modified LUS scores as the strongest predictor of CTD-ILD (OR = 2.79, 95% CI 1.49–5.24; $P = 0.001$), surpassing CT-based metrics such as $LAA_{-600\sim-250}\%$ (OR = 1.66) and TAV/TNV (OR = 0.92). After adjustment for confounders (age, gender, and BMI), modified LUS scores maintained their robust predictive value (aOR = 2.79, 95% CI 1.44–5.44; $P = 0.002$), while $LAA_{-600\sim-250}\%$ and TAV/TNV showed attenuated but still significant associations ($P < 0.05$). Notably, in the fully adjusted model controlling for age, gender, BMI, smoking, disease duration, complications, and CTD type, the association of the modified LUS scores was further strengthened (aOR = 3.62, 95% CI 1.58–8.29; $P = 0.002$), demonstrating its superior and independent predictive power (Table 5).

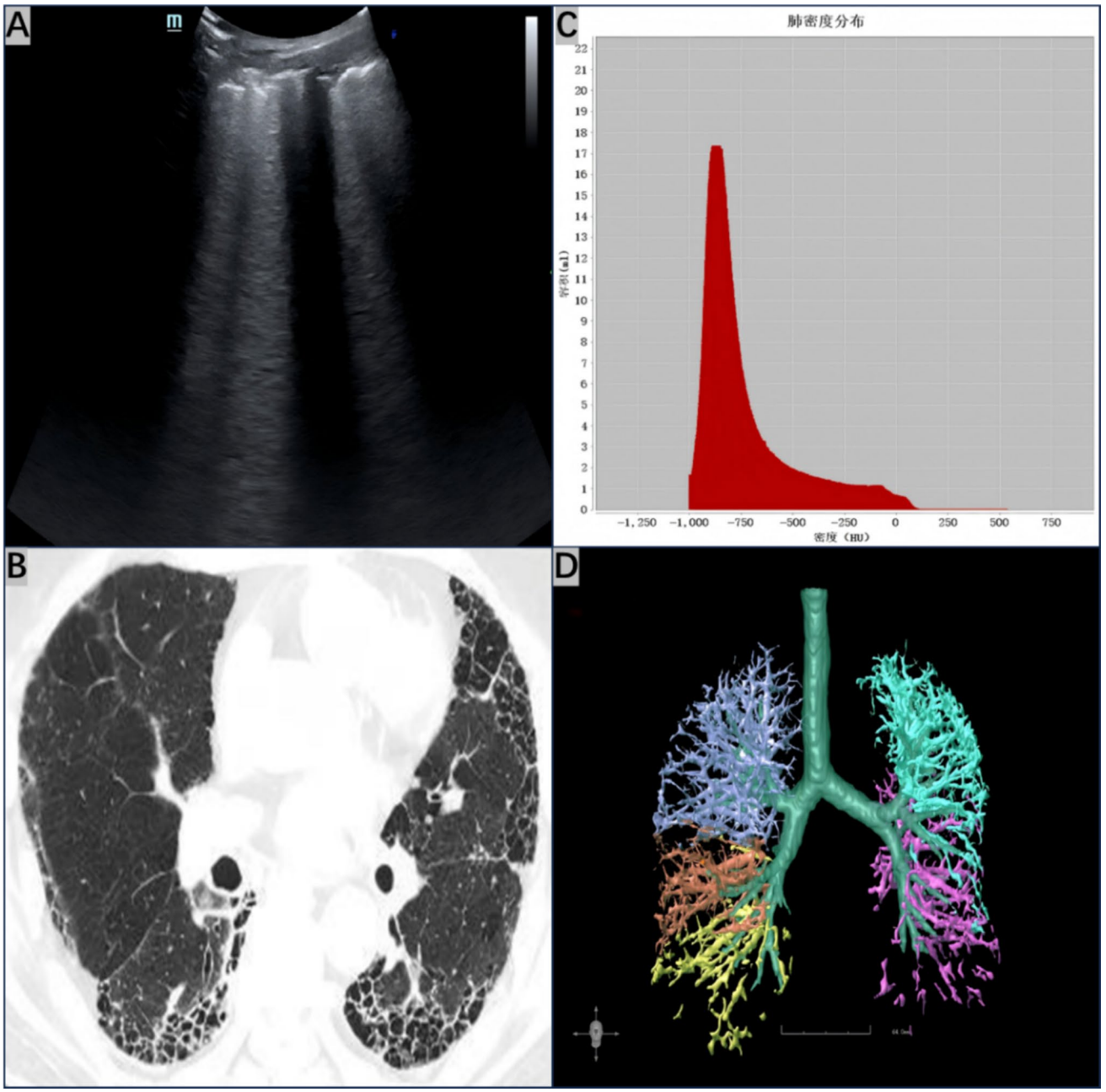

Fig. 2 Images of LUS, HRCT, and QCT in a CTD patient with ILD. **A**–**D** CTD-ILD case: **A** B-lines (arrows) and fragmented pleura on LUS, **B** HRCT showing reticulation and honeycombing, and **C**, **D** QCT demonstrating abnormal attenuation profiles and vascular pruning. CTD, connective tissue disease; ILD, interstitial lung disease; LUS, lung ultrasound; HRCT, high-resolution CT; QCT, quantitative CT

ROC analysis confirmed that both modified LUS scores and $LAA_{-600\sim-250}\%$ were superior discriminators of CTD-ILD (AUC > 0.85), with modified LUS scores demonstrating higher specificity (82% vs. 75%) at matched sensitivity (88%) (Fig. 3). The DeLong test revealed that the modified LUS score demonstrated a significantly higher AUC than the $LAA_{-600\sim-250}\%$ parameter ($P = 0.040$) (Table 6).

Discussion

CTD demonstrates a marked female predominance. A 20-year epidemiological cohort study on mixed CTD by Ungprasert et al. in the USA reported that female patients accounted for 84% of the study population [27]. Our findings revealed a similar female predominance (73.3%),

Table 5 Unadjusted and adjusted oddsratios of per 1/10 SD increase of modified LUS scores, $LAA_{-600\sim-250}\%$, and TAV/TNV analyzed by logistic regression analysis

	Univariable, odds ratio (95% CI)	*P* value
Univariate parameters		
Modified LUS scores	2.792 (1.488, 5.239)	0.001
$LAA_{-600\sim-250}\%$	1.658 (1.221, 2.252)	0.001
TAV/TNV	0.924 (0.873, 0.977)	0.006
Multivariate parameters adj[a]		
Modified LUS scores	2.794 (1.435, 5.437)	0.002
$LAA_{-600\sim-250}\%$	1.746 (1.249, 2.442)	0.001
TAV/TNV	0.936 (0.882, 0.993)	0.028
Multivariate parameters adj[b]		
Modified LUS scores	3.617 (1.578, 8.292)	0.002
$LAA_{-600\sim-250}\%$	1.728 (1.226, 2.437)	0.020
TAV/TNV	0.931 (0.876, 0.989)	0.021

$LAA_{-600\sim-250}\%$ percentage of lung volume with CT number from − 600 to − 250 HU in the total lung volume, *TAV/TNV* the ratio of lumen area to number of blood vessels around the bronchus with a diameter of 2 mm in the lower lobe of the lung, *LUS* lung ultrasound

[a]Adjusted for age, gender, and BMI

[b]Adjusted for age, gender, BMI, smoking, duration, complication, and type of CTD

consistent with established epidemiological trends. Given the chronic progression of these diseases, long-term follow-up is often necessary. During such follow-ups, repeated radiographic examinations pose significant health risks, particularly due to cumulative radiation exposure, which is of particular concern for women of reproductive age. This study innovatively developed a radiation-optimized diagnostic protocol through the retrospective analysis of HRCT data, which avoids additional radiation exposure, in combination with prospective longitudinal LUS assessments. Our findings confirm the initial hypothesis that the modified LUS scores serve as a robust and independent predictor of CTD-ILD. Furthermore, they support the role of LUS as an effective tool in the long-term management of this condition.

Although LUS has demonstrated diagnostic potential for ILD in previous studies [8, 28, 29], two critical limitations persist in the current research. First, standardized scanning protocols are lacking, with protocols ranging from comprehensive 56-intercostal space examinations [28] to simplified 8-zone approaches [30]. Second, existing scoring systems tend to be fragmented, mainly focusing either on B-line quantification or pleural line abnormalities. The modified ultrasound scoring system proposed by Zhang et al., which integrates pleural line characteristics, parenchymal alterations, and complication assessments, has shown diagnostic performance comparable to HRCT Warrick scores (Fig. 4). Building on this system, we optimized the conventional 16-zone protocol into a more clinically practical 12-zone scheme [31–34], with each zone independently scored and summed for total evaluation. This modified approach ensures complete lung coverage while reducing examination time and minimizing patient exposure, striking an optimal balance between clinical feasibility and comprehensive assessment. ROC curve analysis revealed that modified LUS scores had superior diagnostic accuracy compared to isolated B-line scoring and pleural line scoring. Importantly, modified LUS scores showed a strong correlation with disease severity and demonstrated substantial agreement with Warrick scoring in stratifying mild, moderate, and severe ILD. These findings underline modified LUS scores as a reliable imaging biomarker for disease staging and prognostic evaluation in ILD management.

This study pioneers an innovative comparative analysis of modified LUS scores against both HRCT and QCT. QCT enables the objective assessment of fibrosis progression in ILD by quantifying parenchymal parameters [35] and radiation attenuation characteristics. Structural alterations caused by diffuse lesions significantly modify lung tissue density distribution, enabling sensitive detection of fibrotic progression through calculating the percentage of lung volume within the − 600 to − 250 HU attenuation threshold [18]. Notably, this study also innovatively incorporates peripheral pulmonary vascular metrics: fibrosis-induced volume reduction via scar formation and restrictive ventilatory impairment, leading to inadequate inspiration, prompted the selection of bronchus-associated peripheral vasculature as anatomical landmarks. The calculated TAV/TNV ratio further enhanced ILD differentiation. ROC curve analysis demonstrated that modified LUS scores exhibited superior diagnostic performance compared to $LAA_{-600\sim-250}\%$, closely approaching the diagnostic efficacy of HRCT, with higher sensitivity. These findings substantiate modified LUS scores as a feasible diagnostic tool for ILD, offering a comprehensive and precise evaluation of disease severity through its multidimensional scoring architecture.

This study has several limitations. First, the relatively small sample size from a single-center inpatient setting and the lack of stratified analysis across CTD subtypes may limit the generalizability of our findings, particularly for outpatients or those with early or asymptomatic disease. Second, the retrospective acquisition of CT scans and the exclusion of technically incompatible studies may have introduced selection bias, potentially elevating the baseline risk of ILD in the enrolled cohort and influencing the predictive values of the diagnostic parameters. Additionally, although patients with significant cardiorenal comorbidities were excluded,

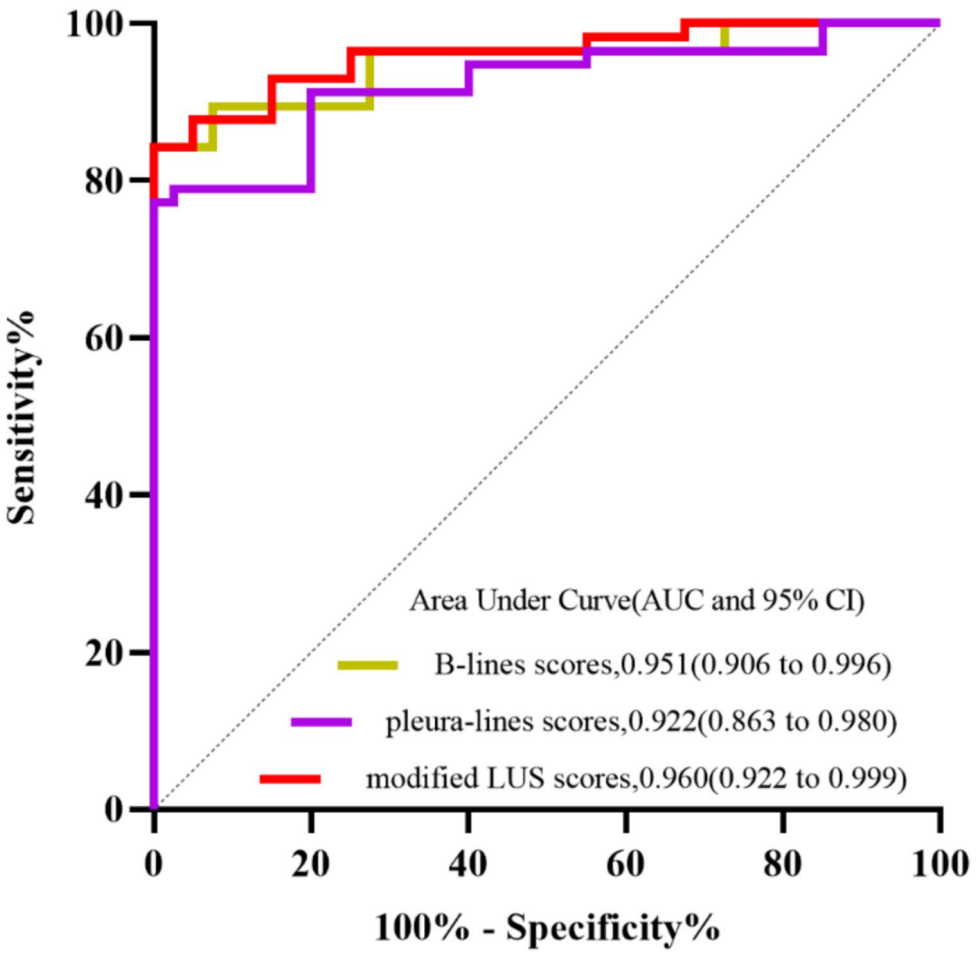

Fig. 3 ROC analysis of ultrasound scoring systems. Modified LUS composite scores (AUC = 0.92, 0.86–0.98) outperformed isolated B-line (0.85, 0.76–0.94) and pleural line (0.81, 0.71–0.91) scores for CTD-ILD detection. AUC values with 95% CIs shown

Table 6 Pairwise comparison of diagnostic performance: LUS parameters vs. QCT using DeLong test for AUC differences

Test result pair	AUC difference	95% CI		*P*
		Lower bound	Upper bound	
B-lines scores vs. pleura-lines scores	0.030	−0.033	0.092	0.351
B-lines scores vs. modified LUS scores	−0.009	−0.047	0.030	0.655
B-lines scores vs. $LAA_{-600\sim-250}\%$	0.078	−0.003	0.159	0.060
Pleura-lines scores vs. modified LUS scores	−0.039	−0.071	−0.006	0.020
Pleura-lines scores vs. $LAA_{-600\sim-250}\%$	0.048	−0.048	0.145	0.326
Modified LUS scores vs. $LAA_{-600\sim-250}\%$	0.087	0.004	0.170	0.040

LUS lung ultrasound, $LAA_{-600\sim-250}\%$ percentage of lung volume with CT number from −600 to −250 HU in the total lung volume

the inherent technical limitations of lung ultrasound persist—B-lines are not specific to fibrosis and can also occur in other pulmonary conditions such as edema or inflammation, which may confound the interpretation of results. Future multicenter studies involving larger and more diverse cohorts, including outpatient populations, are warranted to validate and extend our findings.

However, the study's methodological rigor merits emphasis. Two blinded operators performed quantitative and qualitative LUS assessments using a standardized evidence-based scoring system with uniform machine settings, complemented by QCT texture analysis and multivariable adjustment models, ensuring result reproducibility and reliability. While HRCT remains the gold standard for evaluating parenchymal involvement in CTD-ILD, LUS demonstrates unique clinical advantages in radiation-sensitive populations (e.g., young women, children, and pregnant individuals) due to its radiation-free nature, procedural simplicity, and bedside repeatability. Theoretically, LUS could serve as a first-line imaging modality for suspected CTD-ILD cases.

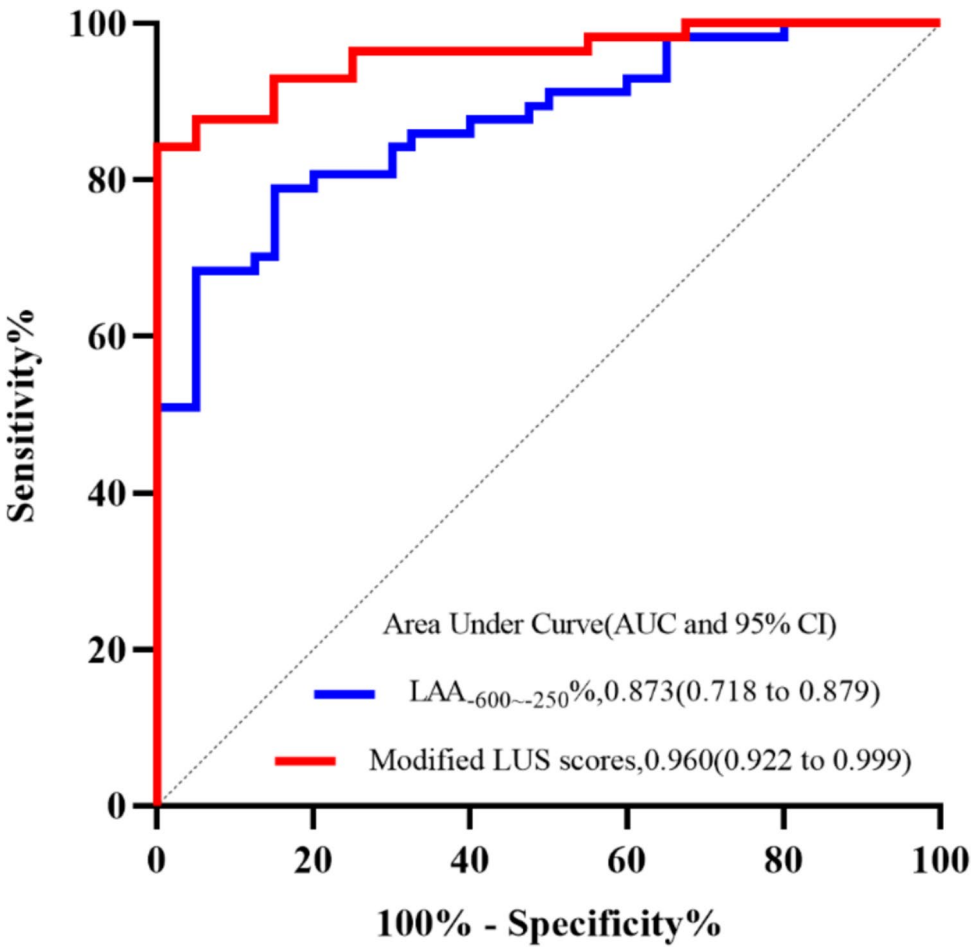

Fig. 4 Diagnostic performance comparison for CTD-ILD. Modified LUS scores (AUC = 0.92) showed superior discrimination versus QCT parameters: $LAA_{-600\sim-250}\%$ (0.82) and TAV/TNV ratio (0.75). $LAA_{-600\sim-250}\%$: − 600 to − 250 HU lung volume percentage. TAV/TNV, vessel area-to-count ratio; LUS, lung ultrasound; $LAA_{-600\sim-250}\%$, percentage of lung volume with CT number from − 600 to − 250 HU in the total lung volume

Future multicenter studies employing standardized protocols are warranted to establish its role in disease stratification and longitudinal monitoring.

Supplementary information The online version contains supplementary material available at https://doi.org/10.1007/s10067-025-07910-1.

Funding This work was supported by the Scientific Research Project of the Education Department of Shaanxi Province (No. 24JK0401) and the Scientific Research Project of the Education Department of Shaanxi Province (No. 24JP049).

Data availability Data generated or analyzed during the study are available from the corresponding author by request.

Compliance with ethical standards

Ethical approval The study protocol was approved by the Ethics Committee of the Affiliated Hospital of Shaanxi University of Chinese Medicine (Approval No. SZFYIEC-BA-2024–20).

Disclosures None.

References

1. Jeganathan N, Sathananthan M (2020) Connective tissue disease-related interstitial lung disease: prevalence, patterns, predictors, prognosis, and treatment. Lung 198(5):735–759
2. Agarwal M, Gupta ML, Deokar K, Shadrach BJ, Bharti N, Sonigra M (2021) Clinico-radiological profile of connective tissue disease related-interstitial lung diseases from a tertiary care centre of India: a cross sectional study. Monaldi archives for chest disease = Archivio Monaldi per le malattie del torace. 91(4)
3. Huang S, Guo R, Yuan X et al (2022) Evaluation of connective tissue disease-related interstitial lung disease using ultrasound elastography: a preliminary study. Quant Imaging Med Surg 12(7):3778–3791
4. Togizbayev G, Shametekov I, Maksot D et al (2025) Biologic therapy in rheumatology: analysis of multidisciplinary teams' performance in Kazakhstan. Int J Rheum Dis 28(6):e70304
5. Togizbayev G, Abdaliev K, Imangaliev E, Bultakova B, Razikhova A (2025) Development of rheumatology services in Atyrau Region, Kazakhstan. Rheumatology (Oxford) 64(6):4065–4066
6. Hassan RI, Lubertino LI, Barth MA et al (2019) Lung ultrasound as a screening method for interstitial lung disease in patients with systemic sclerosis. JCR J Clin Rheumatol 25(7):304–307

7. Rajan SK, Cottin V, Dhar R et al (2023) Progressive pulmonary fibrosis: an expert group consensus statement. Eur Respir J. https://doi.org/10.1183/13993003.03187-2021
8. Tardella M, Di Carlo M, Carotti M, Filippucci E, Grassi W, Salaffi F (2018) Ultrasound B-lines in the evaluation of interstitial lung disease in patients with systemic sclerosis: cut-off point definition for the presence of significant pulmonary fibrosis. Medicine 97(18):e0566
9. Mena-Vázquez N, Jimenez-Núñez FG, Godoy-Navarrete FJ et al (2021) Utility of pulmonary ultrasound to identify interstitial lung disease in patients with rheumatoid arthritis. Clin Rheumatol 40(6):2377–2385
10. Bruni C, Mattolini L, Tofani L et al (2022) Lung ultrasound B-lines in the evaluation of the extent of interstitial lung disease in systemic sclerosis. Diagnostics. https://doi.org/10.3390/diagnostics12071696
11. Watanabe S, Yomono K, Yamamoto S, Suzuki M, Gono T, Kuwana M (2024) Lung ultrasound in the assessment of interstitial lung disease in patients with connective tissue disease: performance in comparison with high-resolution computed tomography. Mod Rheumatol 35(1):79–87
12. Gargani L, Romei C, Bruni C et al (2022) Lung ultrasound B-lines in systemic sclerosis: cut-off values and methodological indications for interstitial lung disease screening. Rheumatology (Oxford, England) 61(Si):Si56-si64
13. Pinal-Fernandez I, Pallisa-Nuñez E, Selva-O'Callaghan A et al (2015) Pleural irregularity, a new ultrasound sign for the study of interstitial lung disease in systemic sclerosis and antisynthetase syndrome. Clin Exp Rheumatol 33(4 Suppl 91):S136-141
14. Rotondo C, Busto G, Rella V et al (2025) Transthoracic lung ultrasound in systemic sclerosis-associated interstitial lung disease: capacity to differentiate chest computed-tomographic characteristic patterns. Diagnostics. https://doi.org/10.3390/diagnostics15040488
15. Buda N, Piskunowicz M, Porzezińska M, Kosiak W, Zdrojewski Z (2016) Lung ultrasonography in the evaluation of interstitial lung disease in systemic connective tissue diseases: criteria and severity of pulmonary fibrosis - analysis of 52 patients. Ultraschall in der Medizin (Stuttgart, Germany : 1980) 37(4):379–385
16. Zhang Y, Lian X, Huang S et al (2023) A study of the diagnostic value of a modified transthoracic lung ultrasound scoring method in interstitial lung disease. Quant Imaging Med Surg 13(2):946–956
17. Bruni C, Occhipinti M, Pienn M et al (2023) Lung vascular changes as biomarkers of severity in systemic sclerosis-associated interstitial lung disease. Rheumatology (Oxford, England) 62(2):696–706
18. Alevizos MK, Danoff SK, Pappas DA et al (2022) Assessing predictors of rheumatoid arthritis-associated interstitial lung disease using quantitative lung densitometry. Rheumatology (Oxford, England) 61(7):2792–2804
19. van den Hoogen F, Khanna D, Fransen J et al (2013) 2013 classification criteria for systemic sclerosis: an American College of Rheumatology/European League Against Rheumatism collaborative initiative. Ann Rheum Dis 72(11):1747–1755
20. Aletaha D, Neogi T, Silman AJ et al (2010) 2010 rheumatoid arthritis classification criteria: an American College of Rheumatology/European League Against Rheumatism collaborative initiative. Arthritis Rheum 62(9):2569–2581
21. Aringer M, Costenbader K, Daikh D et al (2019) 2019 European League Against Rheumatism/American College of Rheumatology classification criteria for systemic lupus erythematosus. Ann Rheum Dis 78(9):1151–1159
22. Shiboski CH, Shiboski SC, Seror R et al (2017) 2016 American College of Rheumatology/European League Against Rheumatism classification criteria for primary Sjögren's syndrome: a consensus and data-driven methodology involving three international patient cohorts. Arthritis & Rheumatology 69(1):35–45
23. Lundberg IE, Tjärnlund A, Bottai M et al (2017) 2017 European League Against Rheumatism/American College of Rheumatology classification criteria for adult and juvenile idiopathic inflammatory myopathies and their major subgroups. Arthritis Rheumatol 69(12):2271–2282
24. Warrick JH, Bhalla M, Schabel SI, Silver RM (1991) High resolution computed tomography in early scleroderma lung disease. J Rheumatol 18(10):1520–1528
25. Karadag DT, Dogan S, Gokcen N, Cagdas OS, Yazici A, Cefle A (2025) Warrick score in rheumatoid-arthritis interstitial lung disease: a promising tool for assessing the extent and progression of lung involvement. Adv Rheumatol 65(1):5
26. Lederer DJ, Enright PL, Kawut SM et al (2009) Cigarette smoking is associated with subclinical parenchymal lung disease: the multi-ethnic study of atherosclerosis (MESA)-lung study. Am J Respir Crit Care Med 180(5):407–414
27. Ungprasert P, Crowson CS, Chowdhary VR, Ernste FC, Moder KG, Matteson EL (2016) Epidemiology of mixed connective tissue disease, 1985–2014: a population-based study. Arthritis Care Res 68(12):1843–1848
28. Pitsidianakis G, Vassalou EE, Vasarmidi E et al (2022) Performance of lung ultrasound for monitoring interstitial lung disease. J Ultrasound Med 41(5):1077–1084
29. Huang Y, Liu T, Huang S et al (2023) Screening value of lung ultrasound in connective tissue disease related interstitial lung disease. Heart Lung 57:110–116
30. Leidi A, Soret G, Mann T et al (2022) Eight versus 28-point lung ultrasonography in moderate acute heart failure: a prospective comparative study. Intern Emerg Med 17(5):1375–1383
31. Haurylenka D, Damantsevich V, Filustsin A, Damantsevich A (2021) Diagnostic value of 12-zone lung ultrasound protocol for diagnosing COVID-19-associated pneumonia in outpatients. J Ultrasonography 21(87):e271–e276
32. Huang P, Chen D, Liu X, Zhang X, Song X (2024) Diagnostic value of bedside lung ultrasound and 12-zone score in the 65 cases of neonatal respiratory distress syndrome and its severity. Biomed Eng Online 23(1):29
33. Han S, Ji Z, Liu Y (2024) Screening value of lung ultrasound and pleural shear wave elastography in connective tissue disease-related interstitial lung disease: a preliminary study. Clin Rheumatol 43(6):2117–2123
34. Mancusi C, Giallauria F, Piccoli M et al (2025) Lung ultrasound in cardiac rehabilitation: expert consensus on protocols, clinical use, and integration into patient management from the working group on cardiac rehabilitation and cardiovascular prevention of the Italian society of cardiology. Heart Fail Rev 30(6):1423–1433
35. Pu D, Yuan H, Ma G, Duan H, Zhang M, Yu N (2023) CT quantitative analysis of pulmonary changes in rheumatoid arthritis. J X-ray Sci Technol 31(3):545–553

Publisher's Note Springer Nature remains neutral with regard to jurisdictional claims in published maps and institutional affiliations.

Springer Nature or its licensor (e.g. a society or other partner) holds exclusive rights to this article under a publishing agreement with the author(s) or other rightsholder(s); author self-archiving of the accepted manuscript version of this article is solely governed by the terms of such publishing agreement and applicable law.

Authors and Affiliations

Xiaokun Xin[1] · Meng Huang[2] · Hui Yuan[3] · Li Zhang[1] · Shan Dang[4] · Guoqin Huang[2] · Nan Yu[1,4]

✉ Nan Yu
yunan0512@sina.com

[1] School of Medical Technology, Shaanxi University of Chinese Medicine, Xixian Avenue, Fengxi New City, Xixian New Area, Xian Yang, Shaanxi Province 712046, China

[2] Department of Ultrasound Medicine, Affiliated Hospital of Shaanxi University of Chinese Medicine, Xianyang, China

[3] Department of Rheumatology Immunohematology, Affiliated Hospital of Shaanxi University of Chinese Medicine, Xianyang, China

[4] Department of Medical Imaging, Affiliated Hospital of Shaanxi University of Chinese Medicine, Xianyang, China